Critical currents in ballistic two-dimensional InAs-based superconducting weak links

Heida, J.P.; Wees, B.J. van; Klapwijk, T.M.; Borghs, G.

Link to publication in University of Groningen/UMCG research database

Critical currents in ballistic two-dimensional InAs-based superconducting weak links

J. P. Heida, B. J. van Wees, and T. M. Klapwijk

Department of Applied Physics and Material Science Centre, University of Groningen, Nijenborgh 4,
9747 AG Groningen, The Netherlands

G. Borghs

Interuniversity Microelectronics Centre, Kapeldreef 75, B-3030, Leuven, Belgium
(Received 4 January 1999; revised manuscript received 4 August 1999)

The critical supercurrent I_c carried by a short (0.3 to 0.8 μm) *ballistic* two-dimensional InAs-based electron gas between superconducting niobium electrodes is studied. In relating the maximum value to the resistance of the weak link in the normal state R_n a much lower value is found than theoretically expected for a ballistic system. The energy scale which characterizes the observed temperature dependence is comparable to the energy associated with the product of I_c and R_n. We point out that although the transport between the electrodes is ballistic, in the InAs underneath the superconducting electrodes the transport is diffusive, an experimental case which has not yet been studied theoretically. [S0163-1829(99)09741-6]

Supercurrents in ballistic superconductor–normal-metal–superconductor (*SNS*) structures are microscopically due to Andreev bound states. The pairing interaction which leads to an energy gap of Δ around the Fermi energy E_F in the superconductor (*S*) is absent in the normal material (*N*) and the normal electrons are communicating with the superconductors via Andreev reflection.[1] If an electron with wave number $k_e = k_F + E/\hbar v_F$ (with E the energy from E_F, and v_F the Fermi velocity) Andreev reflects, a Cooper pair is formed in the superconductor and a hole with wave vector $k_h = k_F - E/\hbar v_F$ is reflected into the normal region. The dynamical phase acquired by the incoming electron is therefore opposite to the dynamical phase acquired by the retroreflected hole which travels back along the same path. Such phase conjugated closed trajectories of electrons and holes coupled via Andreev reflections lead to a discrete set of energy levels at energies which are dependent on the difference of the macroscopic phases of the superconductors. A supercurrent can flow through these bound states. Using these concepts the maximum supercurrent I_c can be calculated[2-11] and related to the normal state resistance R_n of the weak link. Experimentally (see Fig. 1) we find that the $I_c R_n$ product, which is independent of the width of the device, is much lower than theoretically predicted. These *low* values are the most prominent deviation from theory for samples that are experimentally in the required ballistic limit.[12-20]

For short junctions where the junction length $L \ll \xi_0 = \hbar v_F/2\Delta$ so that $(k_e - k_h)L \approx 0$ there is only one bound state per mode in the energy window $E_F \pm \Delta$. At $T=0$, the $I_c R_n$ product is $\pi\Delta/e$. The theory describing such ballistic short junctions is known as KO I (after Kulik and Omelyanchuk[4]). The associated temperature dependence of the critical current is shown in Fig. 2. If intermode scattering is introduced in the normal region between the two superconductors, one can calculate the average $I_c R_n$ product for such a diffusive system. Kulik and Omelyanchuk[4] find that $\langle I_c \rangle \langle R_n \rangle = 0.66\pi\Delta/e$ (KO II). For comparison, for a tunnel junction the Ambegaokar-Baratoff result gives $\pi\Delta/2eR_n$. For this short junction limit the temperature dependence of the three different cases is illustrated in Fig. 2.

For longer junctions, the energy scale that sets the $I_c R_n$ product is not Δ but the Thouless energy E_{Th}.[21,22] The Thouless energy is related to the electron dwell time in the junction. For a diffusive system it is $E_{Th,d} = \hbar D/L^2$ with D the diffusion constant. For a ballistic system it is $E_{Th,b} = \hbar v_F/L$. The distinction between long and short is set by the ratio of the Thouless energy compared to the energy gap Δ. For temperatures $k_B T > E_{Th}$, the associated temperature dependence of the critical current is $\exp(-\sqrt{k_B T/E_{Th,b}})$ and $\exp(-k_B T/E_{Th,b})$ for the diffusive and the ballistic cases, respectively.

A schematic figure and a scanning electron micrograph of the sample are shown in Fig. 3. The Nb electrodes are coupled by a two-dimensional electron gas (2DEG) in a 15 nm thick InAs quantum well (QW) between AlSb barriers. To produce the sample a mesa etch pattern is first written in PMMA using electron beam lithography (EBL). This pattern is transferred to the heterostructure by wet etching of the AlSb top layer and the InAs quantum well. Secondly, the electrode pattern is defined in PMMA with EBL and the AlSb top layer is removed by chemical wet etching to expose the InAs QW. Finally the sample is loaded in a UHV chamber where the InAs QW surface is cleaned with a 500 eV Ar-ion bombardment prior to deposition of 70 nm thick Nb electrodes.

Four junctions were prepared on the same chip of InAs in the same production batch. The mesa etch width is W $=0.7$ μm. The Nb-2DEG contact is made in the dark region in Fig. 3 (indicated as bare InAs under Nb). The interelectrode distance L is the length of the channel between these
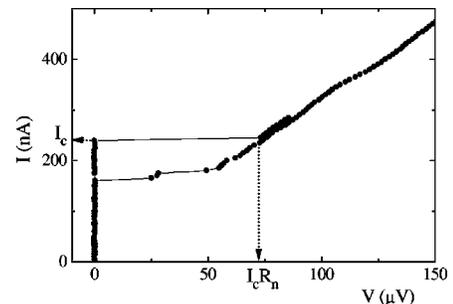

FIG. 1. Current-voltage characteristic for sample No. 4 illustrating the experimental definitions of I_c and $I_c R_n$, indicated by arrows ($T=0.7$ K).
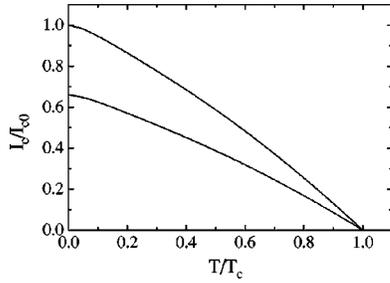
FIG. 2. Critical current as a function of temperature for a short ballistic contact (KO1, top) and a short diffusive contact (KO2, bottom). The supercurrent is normalized to $I_c = \pi\Delta/eR_n$.

regions; it ranges from 0.32 to 0.78 μm. The channel itself is covered with an AlSb top layer to ensure a high mobility, ballistic channel.

The samples have an electron density $n_s = 2.1 \times 10^{16}$ m^{-2} as obtained from Shubnikov–de Haas measurements of the actual sample. Given the mobility of 10 m^2/V s, the mean free path is larger than 1 μm, much longer than the channel length L. The low magnetic field data (Fig. 4) support the assumption that the channel is indeed ballistic. For $B<0.3$ T the differential resistance is modulated by the presence of a supercurrent. The low field magnetoresistance is dominated by magnetic depopulation of the electron modes in the ballistic channel. For low magnetic fields where $l_c \gg \frac{1}{2}W$, with $l_c = \hbar k_F/eB$, the magnetoresistance is given by

$$R = \frac{h}{2e^2}\frac{\pi}{Wk_F} + \frac{\pi^3 W}{12hk_F^3}B^2 \qquad (1)$$
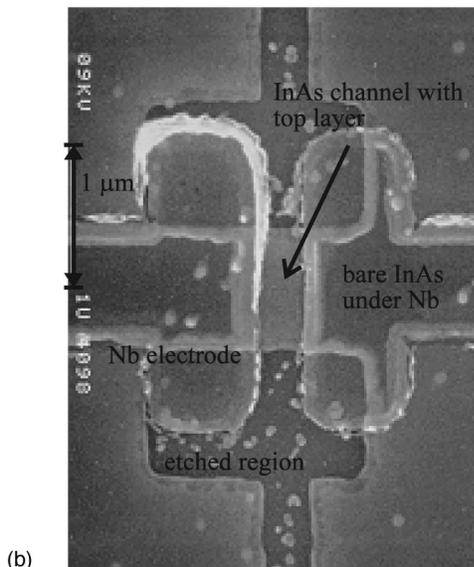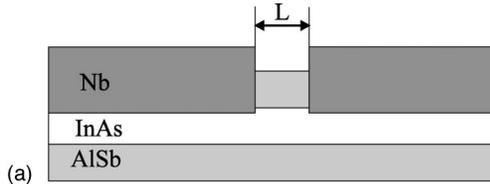

(a)

(b)

FIG. 3. Top: schematic cut through of a sample. Bottom: scanning electron microscope picture of a sample.
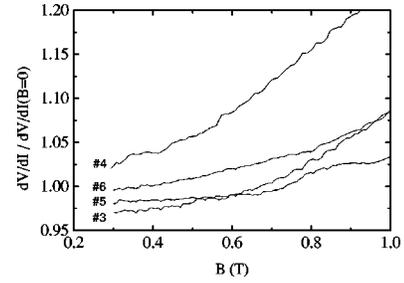

FIG. 4. Magnetoresistance at 4.2 K showing magnetic depopulation of the channel region.

using a Taylor approximation of the number of modes in the two-dimensional electron gas.[23] With the measured values for n_s and W, the parabolic behavior $R = aB^2$ (with $a = \pi^3 W/12hk_F^3$) is expected to have $a \approx 60$. The measured values of a are also given in Table I and are comparable to those expected from the material geometry and material properties: consistent with the assumption that the channel is ballistic. The first term of Eq. (1) is the Sharvin resistance. The measured resistances (see Table I) are higher than the Sharvin resistance $R_{Sh} = (h/2e^2)(\pi/k_F W) = 160\,\Omega$ which we primarily attribute to some remnant scattering at the interfaces. From their low resistance, we conclude that the junctions have highly transparent interfaces which is supported by a decrease in resistance below the superconductor gap due to Andreev reflection.

Both the width and the length of the samples are smaller than the inelastic scattering length of the material, $l_{in} \approx 10$ μm.[24] At the low temperatures used it is also smaller than the thermal coherence length $\xi_T = \hbar v_F/2\pi k_B T \approx 15$ μm (at 0.1 K). Thus the junction length and width are smaller than the phase coherence length $l_\phi = \min(\xi_T, l_{in})$. Moreover, the junction dimensions are comparable to the superconducting coherence length $\xi_0 = \hbar v_F/2\Delta \approx 0.5$ μm (with $\Delta = 1.1$ meV, obtained from the superconducting transition temperature of the Nb), so that they are in between the long ($L \gg \xi_0$) and short ($L \ll \xi_0$) limit.

Thus, the sample is a ballistic channel between two high transparency superconducting electrodes and electrons can travel phase coherently between the electrodes. Therefore in theory the junctions are expected to carry a supercurrent with an $I_c R_n$ product of the order of $\pi\Delta/e$.

The experimentally obtained I_c and $I_c R_n$ values at 0.1 K are given in Table I. The sample leads were filtered by a

TABLE I. Experimental parameters of the junctions. R_n is derived from the slope of the IV curve, a is the coefficient of the parabolic fit to the magnetoresistance between 0.3 and 1.0 T. The critical current I_c is the value measured at $T=0.1$ K. I_c and $I_c R_n$ are determined in the manner indicated in vs. temperature curve shows an exponential decay with coefficient T_0.

Sample	L	R_n	a	I_c	$I_c R_n$	T'	T_0	$k_B T_0/e$
	(μm)	(Ω)	(Ω/T^2)	(nA)	(μV)	(K)	(K)	(μeV)
3	0.32	468	53	79	37	0.25	0.47	41
4	0.47	300	68	260	78	0.25	0.91	78
5	0.63	451	97	62	28	0.25	0.55	43
6	0.78	456	81	80	36	0.30	0.51	44

home made cryogenic filter connected to the mixing chamber of the dilution fridge. The filters contain for each (manganin) lead a three stage low pass RC filter (with very low inductance metal film resistors of 2.7 kΩ and ceramic disc capacitors of 1 nF) after which the leads pass a segment filled with fine Cu powder before connection to the sample electrodes. Without these filters the noise temperature is higher than the bath temperature. In the temperature range used in the experiments (below 2.5 K) the temperature dependence of the superconductor energy gap does not play a role. (The Nb electrodes have a T_c of 7 K, see Fig. 2.) R_n in Table I is the slope of the current voltage characteristic at low voltages. Due to multiple Andreev reflection,[25] this resistance deviates slightly from the normal resistance at voltages $V > 2\Delta/e$ which is the R_n referred to in the theoretical work. In the voltage carrying state, multiple Andreev reflection leads to a smearing of the distribution function.[26] This can effectively be seen as heating. This leads to hysteresis because the supercurrent in the voltage carrying state is lower than the supercurrent through the Andreev bound states which are populated according to the Fermi-Dirac distribution function in the zero voltage state. To describe the hysteresis by the RCSJ model, the needed capacitance is far higher than the capacitance calculated from geometry an upper limit of which is 1 fF, disregarding the fact that the capacitor plates are connected by a conducting channel.[27]

Both the observed values of R_n and $I_c R_n$ do *not* scale with the interelectrode separation L so that from the experiment we expect that the junctions are in the short junction limit. However, the critical current magnitude is much smaller than expected for a junction with transparent interfaces in the short junction limit. Sample No. 4 has a higher $I_c R_n$ product than the three other samples. This is accompanied by a lower normal resistance while the material parameters such as the electron density are identical.

In Fig. 5 the temperature dependence of the critical current is shown. To determine the critical current a dedicated electronic circuit is used. The output is the current at which the voltage across the junction exceeds a minimum voltage (8 μV). For a sharp current voltage characteristic (such as in Fig. 1) this is the critical current. Due to noise the set minimum voltage can be exceeded before the critical current is reached which leads to the noise in I_c in Fig. 5. This noise is more prominent in the panels which show a low I_c. If the current voltage characteristics are rounded due to thermal fluctuations this method cannot be used because the measured output differs from the intrinsic critical current. In this range the critical current is obtained from a fit of the current voltage characteristic to the RSJ model with thermal noise.[28] In apparent contrast to Thomas *et al.*[29] we find, within our measurement accuracy, excellent agreement with this model, which allows us to determine the critical current also at elevated temperatures. Where this method was used, these values are shown as dots in Fig. 5.

All samples show a decay of the critical current with temperature. A temperature T' is defined above which this decay is faster than below. T' is approximately 0.3 K (see Table I). Over the range measured the critical current does not saturate down to the lowest temperature. The observed $I_c(T)$ has a negative curvature for $T > T'$ whereas theoretically, for small junctions the curvature is positive over the entire temperature
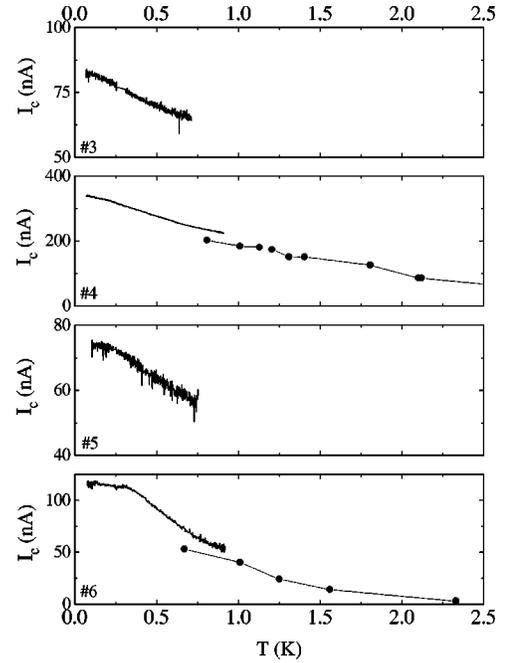

FIG. 5. Supercurrent versus temperature. The dots are values determined from the IV characteristic and the RSJ model with thermal noise.

range irrespective of junction transparency.[11] In the concave region the data can be fitted well with an exponential decay [$I_c \propto \exp(-T/T_0)$]. The temperature range T_0 over which I_c decreases with a factor e is also tabulated in Table I. The junctions A, C, and D have, within the fitting accuracy, identical T_0 irrespective of their length. We note that for samples Nos. 3 and 6 this is a property shared with their $I_c R_n$ product. Junction B shows a doubling of both the $I_c R_n$ product and the decay temperature T_0. The range over which the fit to an exponential decay is performed is not very large but shows that the characteristic decay temperature T_0 is comparable to, and seems directly related to the $I_c R_n$ product of the junctions.

This case, intermediate between ballistic and diffusive has not been studied theoretically. However, we like to point out that also in the case of diffusive transport in our group we have not been able to obtain quantitative agreement between theory and experiment in particular for the case of sample specific fluctuations.[30]

The most prominent observation here is the low $I_c R_n$ product. We find that both the critical current magnitude and its I_c vs temperature curve are independent of the junction length. Sample No. 4 has a higher $I_c R_n$ product and a higher decay temperature T_0 accompanied by a lower normal resistance R_n. We find (Table I) that the energy scales of the three measured parameters $I_c R_n$ and T_0 are comparable. Also, the energy scale of T' is of the same order of magnitude. Interpretation of these temperatures as a Thouless energy setting the scale of the $I_c R_n$ product for a long junction would mean either a low diffusion constant D or an effective junction length L of about ten times its physical length. Both are incompatible with the ballisticity of the channel.

A possible origin of the low supercurrent may be scattering introduced by Ar etching of the InAs surface prior to Nb deposition. The ion bombardment, intended to remove the

native oxide, also modifies the region under the Nb contact. Locally the bombardment reduces the electron mean free path to approximately 10 nm and induces a high electron density so that the interface is nonspecular.[31] Whereas for Andreev reflection from a specular interface, the hole is ret-roreflected and has the same wavevector as the incoming electron from which it originates, the reflected hole from a diffusive interface has partial waves in all directions.[32] A rough estimate of this effect yields a depressed $I_c R_n$ product comparable to the measured result. To form an Andreev bound state, the electron or hole should still be in the same mode after two Andreev reflections the probability of which is $1/N^2$ with fully diffusive Andreev reflection where the Andreev reflected quasiparticle in mode i is distributed over all modes $0\cdots N$. Consequently, the supercurrent for the N-mode wide junction would be depressed by a factor $N/N^2 = 1/N = 1/30$.

Volkov et al.[33] have shown theoretically that the electronic states in the InAs quantum well under the Nb electrode with a highly transparent interface have an effective excitation gap. Its magnitude is comparable to the Nb superconducting gap and the electrons from the channel Andreev

reflect of this induced excitation gap. The presented experimental work does not support the presence of this gap in the studied sample. Maybe the prerequisite of adiabaticity is not fully satisfied in our samples.

In conclusion, we have observed that the supercurrent in ballistic mesoscopic Josephson junctions is at least an order of magnitude smaller than expected from theory which assumes ideal boundaries. We have found that the $I_c R_n$ product, the temperature T' above which $I_c(T)$ decreases exponentially, and T_0, the decay temperature of this exponential decrease have a comparable energy scale. For our well characterized junctions with ballistic channels, the disordered region under the Nb contacts may well cause the lowered $I_c R_n$ products observed.

[1] A. F. Andreev, Zh. Eksp, Teor. Fiz. **46**, 1823 (1964) [Sov. Phys. JETP **19**, 1228 (1964)].
[2] I. O. Kulik, Zh. Éksp. Teor. Fiz. **57**, 1745 (1969) [Sov. Phys. JETP **30**, 944 (1970)].
[3] J. Bardeen and J. L. Johnson, Phys. Rev. B **5**, 72 (1972).
[4] I. O. Kulik and A. N. Omelyanchuk, Fiz. Nizk. Temp. **3**, 945 (1977) [Sov. J. Low Temp. Phys. **3**, 459 (1977)].
[5] K. K. Likharev, Rev. Mod. Phys. **51**, 101 (1979).
[6] A. Furusaki and M. Tsukada, Phys. Rev. B **43**, 10 164 (1991).
[7] C. W. J. Beenakker and H. van Houten, Phys. Rev. Lett. **66**, 3056 (1991).
[8] P. F. Bagwell, Phys. Rev. B **46**, 12 573 (1992).
[9] C. W. J. Beenakker, in *Transport Phenomena in Mesoscopic Systems*, edited by H. Fukuyama and T. Ando, Springer Series in Solid-State Sciences Vol. 109 (Springer, Berlin, 1992), p. 235.
[10] U. Schüssler and R. Kümmel, Phys. Rev. B **47**, 2754 (1993).
[11] A. Chrestin, T. Matsuyama, and U. Merkt, Phys. Rev. B **49**, 498 (1994).
[12] J. Nitta, T. Akazaki, H. Takayanagi, and K. Arai, Phys. Rev. B **46**, 14 286 (1992).
[13] H. Takayanagi and T. Akazaki, Solid State Commun. **96**, 815 (1995).
[14] L. C. Mur et al., Phys. Rev. B **54**, R2327 (1996).
[15] H. Kroemer et al., Physica B **203**, 298 (1994).
[16] H. Takayanagi, T. Akazaki, and J. Nitta, Phys. Rev. B **51**, 1374 (1995).
[17] H. Takayanagi, T. Akazaki, and J. Nitta, Phys. Rev. Lett. **75**, 3533 (1995).
[18] H. Takayanagi, J. B. Hansen, and J. Nitta, Physica B **203**, 291 (1994).
[19] B. J. van Wees, P. H. C. Magnee, J. P. Heida, A. Dimoulas, and T. M. Klapwijk, Physica B **203**, 285 (1994).
[20] A. Chrestin, T. Matsuyama, and U. Merkt, Phys. Rev. B **55**, 8457 (1997).
[21] F. K. Wilhelm, A. D. Zaikin, and G. Schön, Czech. J. Phys. **46**, 2395 (1996).
[22] F. K. Wilhelm, A. D. Zaikin, and G. Schön, J. Low Temp. Phys. **106**, 305 (1997).
[23] C. W. J. Beenakker and H. van Houten, in *Solid State Physics*, edited by F. Seitz, D. Turnbull, and H. Ehrenreich (Academic Press, New York, 1991), Vol. 44.
[24] A. F. Morpurgo, Ph.D. thesis, University of Groningen, 1998.
[25] T. M. Klapwijk, G. E. Blonder, and M. Tinkham, Physica B & C **109&110B**, 1657 (1982).
[26] K. Flensberg, J. B. Hansen, and M. Octavio, Phys. Rev. B **39**, 8707 (1989).
[27] The capacitor plates are defined as the entire InAs region bounded by the mesa etch extending 16 μm to each side of the junction in the plane of the junction (b) with a separation (s) of 1 μm of the etched channel between the InAs regions. Thus with $C = (2/\pi)\epsilon_0\epsilon_r \ln[4(s_m/b+1)/(s_m/b-1)]$, where $s+m=s+b$ and $\epsilon_r=7$, the average of vacuum and AlSb we find $C=1.9\times10^{-10}F/m$. The width of the mesastructure is 4.9 μm which yields $C\approx1fF$ [see O. Zinke, *Widerstände, Kondensatoren, Spulen und ihre Werkstoffe* (Springer Verlag, Berlin, 1965)].
[28] V. Ambegaokar and B. I. Halperin, Phys. Rev. Lett. **22**, 1364 (1969).
[29] Thomas et al. (unpublished).
[30] S. G. den Hartog, C. M. A. Kapteyn, B. J. van Wees, T. M. Klapwijk, and G. Borghs, Phys. Rev. Lett. **76**, 4592 (1996); S. G. den Hartog, C. M. A. Kapteyn, B. J. van Wees, T. M. Klapwijk, and G. Borghs, Phys. Rev. B **56**, 13 738 (1997).
[31] P. H. C. Magnee, S. G. den Hartog, B. J. van Wees, T. M. Klapwijk, W. v.d. Graaf, and G. Borghs, Appl. Phys. Lett. **67**, 3569 (1995).
[32] A. F. Morpurgo, S. Holl, B. J. van Wees, T. M. Klapwijk, and G. Borghs, Phys. Rev. Lett. **78**, 2636 (1997).
[33] A. F. Volkov, P. H. C. Magnee, B. J. van Wees, and T. M. Klapwijk, Physica C **242**, 261 (1995).